Journal of Alloys and Compounds, 206 (1994) 147–153
JALCOM 1040

Study of electrical conduction behaviour of the $Sr_{1-x}La_xTi_{1-x}Ni_xO_3$ ($x \leqslant 0.10$) system

Om Parkash[a], Lakshman Pandey[b] and D. Kumar[c]

[a]*School of Materials Science and Technology, Institute of Technology, Banaras Hindu University, Varanasi-221005 (India)*
[b]*Department of Post-Graduate Studies and Research in Physics, Rani Durgawati University, Jabalpur-482001 (M.P.) (India)*
[c]*Department of Ceramic Engineering, Institute of Technology, Banaras Hindu University, Varanasi - 221005 (India)*

(Received September 29, 1993)

Abstract

Electrical conduction behaviour of the $Sr_{1-x}La_xTi_{1-x}Ni_xO_3$ ($x \leqslant 0.10$) system has been studied by complex plane impedance spectroscopy and AC conductivity measurements in the temperature range 300–575 K. Both these studies show that conduction occurs by a Debye-type loss process at low temperatures and by excitation of charge carriers at valence band edge and hopping at energies close to it at high temperature among localized nickel sites mainly responsible for conduction.

1. Introduction

$LaCoO_3$ is a semiconductor which undergoes a semiconductor-to-metal transition at 1210 K [1, 2]. It finds potential applications as a catalyst for oxidation of pollutant gases in automotive exhaust, as an oxygen–air electrode catalyst in zinc–air batteries used in urban transport, as a cathode material in high temperature solid electrolyte (HTSE) fuel cells and as oxygen sensors in pure or doped form [3–6]. Titanates with the general formula, $MTiO_3$ where M ≡ Pb, Ba, Sr and Ca in doped or undoped form are important materials used in a number of electronic devices [7, 8]. For the last few years, we have been exploring the possibility of forming a solid solution between these two types of important useful materials, *i.e.* between $LaCoO_3$ and $MTiO_3$ (M ≡ Pb, Ba, Sr and Ca) and studying their dielectric properties with a view to exploring new materials having useful properties [9–11]. It has been found that a solid solution forms over the extensive ranges of compositions in the $M_{1-x}La_x\ Ti_{1-x}Co_xO_3$ systems (M ≡ Pb, Ba, Sr and Ca). These systems exhibit interesting electrical and dielectric properties. Samples with $x \leqslant 0.50$ exhibit dielectric relaxor behaviour, in the system $Pb_{1-x}La_xTi_{1-x}Co_xO_3$ [9]. Grain boundary barrier layers form in the compositions with $0.20 \leqslant x \leqslant 0.40$ in the system $Sr_{1-x}La_xTi_{1-x}Co_xO_3$ imparting very high values of dielectric constant to the materials [10]. In the $Ba_{1-x}La_xTi_{1-x}Co_xO_3$ system, compositions with $x = 0.01$ and 0.05 exhibit very diffuse ferroelectric to paraelectric transition [11].

The interesting and useful properties of these materials prompted us to extend our studies to analogous systems $M_{1-x}La_xTi_{1-x}Ni_xO_3$ (M ≡ Ba, Sr) [12, 13]. These are solid solutions of $BaTiO_3$ and $SrTiO_3$ with $LaNiO_3$. $LaNiO_3$ exhibits metallic conductivity and Pauli paramagnetism [14]. It has been found that solid solution formation is restricted to only limited ranges of composition [12, 13]. In both the above systems, solid solution forms only up to $x = 0.10$. Dielectric relaxor behaviour is observed in the system $Sr_{1-x}La_xTi_{1-x}Ni_xO_3$ for the samples with $x \geqslant 0.05$ above room temperature (300 K). In this paper we are reporting the electrical conduction behaviour of these materials. The study of conduction behaviour is important as it plays an important role in the dielectric properties.

In order to understand the electrical conduction behaviour of polycrystalline materials, it is necessary to separate the various contributions to the total observed conductivity. There are three contributions, namely,

(a) bulk contribution due to grains known as intragranular conduction,

(b) intergranular contribution due to grain boundaries and

(c) electrode sample interface contribution known as electrode polarization.

Complex plane impedance analysis has been used extensively to separate these contributions in solid electrolytes or fast ion conductors [15, 16]. In this, each of the above contributions is represented by an equivalent circuit containing a resistance, R and a capacitance,

SSDI 0925-8388(93)01040-B

C in parallel. The sample then corresponds to three parallel R–C combinations connected in series. In the complex plane impedance analysis, the imaginary part, Z'' of the total complex impedance Z^* is plotted against the real part Z' over a range of frequencies. If all the three processes mentioned above has single but different values of relaxation times, then in the complex plane impedance plot, one gets three semi-circular arcs with their centres on the Z' axes. The arc with highest frequency range passing through the origin normally represents the bulk effects, that with intermediate frequency range gives the grain boundaries contribution while the arc with lowest frequency range represents the contribution of the electrode specimen interface. Electrode processes being highly capacitive in nature will generally occur only at very low frequencies. The resistance as a result of these contributions are obtained from the intercepts of these arcs on Z' axes. In case there is a distribution of relaxation times instead of a single relaxation time for any of the above processes, then a depressed circular arc with its centre below the Z' axis is observed. Angle α, which the line joining the origin to the centre of the arc makes with Z' axes, is a measure of the distribution of relaxation times for that process [17]. Complex plane impedance analysis has been applied successfully to the semiconducting barium titanate showing positive temperature coefficients of resistance effect to separate the various contributions to the total observed resistance [18]. Recently we have studied the electrical conduction behaviour of the $Ba_{1-x}La_xTi_{1-x}Ni_xO_3$ system [19] using complex plane impedance analysis. In this paper we are reporting the results of our investigations on the $Sr_{1-x}La_xTi_{1-x}Ni_xO_3$ system using this method.

2. Experimental details

All the samples ($x = 0.01$, 0.03, 0.05, 0.10) were prepared by the ceramic method using strontium oxalate, lanthanum oxalate, basic nickel carbonate and TiO_2, all having purity of 99.5% or better. Lanthanum oxalate and strontium oxalate were estimated as lanthanum oxide and strontium carbonate respectively. Appropriate quantities of these materials were weighed and mixed in an agate mortar using acetone. The dried powders were transferred to platinum crucibles and calcined at 1523 K for 12 h and furnace cooled. The calcined powders were ground, mixed with a 1% solution of polyvinyl alcohol as binder and pressed into cylindrical pellets. The pellets were heated slowly to 873 K and kept at this temperature for about 1/2 h to burn off the binder. The temperature was then raised to 1573 K and samples were fired at this temperature for 24 h and then cooled in furnace.

X-ray diffraction (XRD) patterns of the resulting samples were taken using Cu Kα radiation in a Jeol X-ray diffractometer. To measure the capacitance C, conductance G, and dissipation factor D, both surfaces of sintered pellets were polished smooth and coated with air-dried silver paint. The measurements were carried out in the temperature range 300–575 K as a function of frequency (1 KHz to 1 MHz) using an HP 4192A LF impedance analyser. The measurements were made on at least two pellets of each composition during heating as well as cooling.

3. Results and discussion

Compositions with $x = 0.01$, 0.03, 0.05 and 0.10 were found to be single-phase solid solutions as indicated by their powder X-ray diffraction patterns. The absence of diffraction lines characteristic of constituent oxides in the diffraction patterns of these compositions confirmed the formation of solid solutions in them. XRD data of these compositions could be indexed on the basis of a cubic unit cell similar to $SrTiO_3$ [13]. Capacitance and conductance were measured for all the samples at various steady temperatures. Real, Z', and imaginary, Z'', parts of the complex impedance Z^*, were calculated using the relations:

$$Z' = \frac{G}{G^2 + \omega^2 C^2}, \qquad Z'' = \frac{\omega C}{G^2 + \omega^2 C^2} \tag{1}$$

The imaginary part, Z'' was plotted against the real part, Z' over the frequency range 1 KHz–1 MHz. Some typical plots for the samples are shown in Figs. 1 and 2.

In the compositions with $x = 0.01$ and 0.03, one depressed circular arc passing through the origin is observed at low temperatures. Impedance plots for $x = 0.05$ and 0.10 clearly show the presence of two depressed circular arcs, with one passing through the origin. At higher temperatures, two distinct circular arcs are observed in all the samples. The second arc becomes more distinct with increasing temperature, and it is quite likely that a sample with $x = 0.01$ and 0.03 may have another arc in the low frequency range (< 1 KHz) at low temperatures. The values of resistance corresponding to two arcs are obtained by their intersection with the Z' axis. The arc passing through the origin represents the bulk contribution, while the one in the lower frequency range may represent the grain boundaries or specimen electrode contribution to the total observed conduction. Some more experiments are needed to ascertain whether the arc at low frequency in our case is due to the grain boundaries or the electrode–specimen interface contribution. We will discuss only the bulk resistance determined from the high

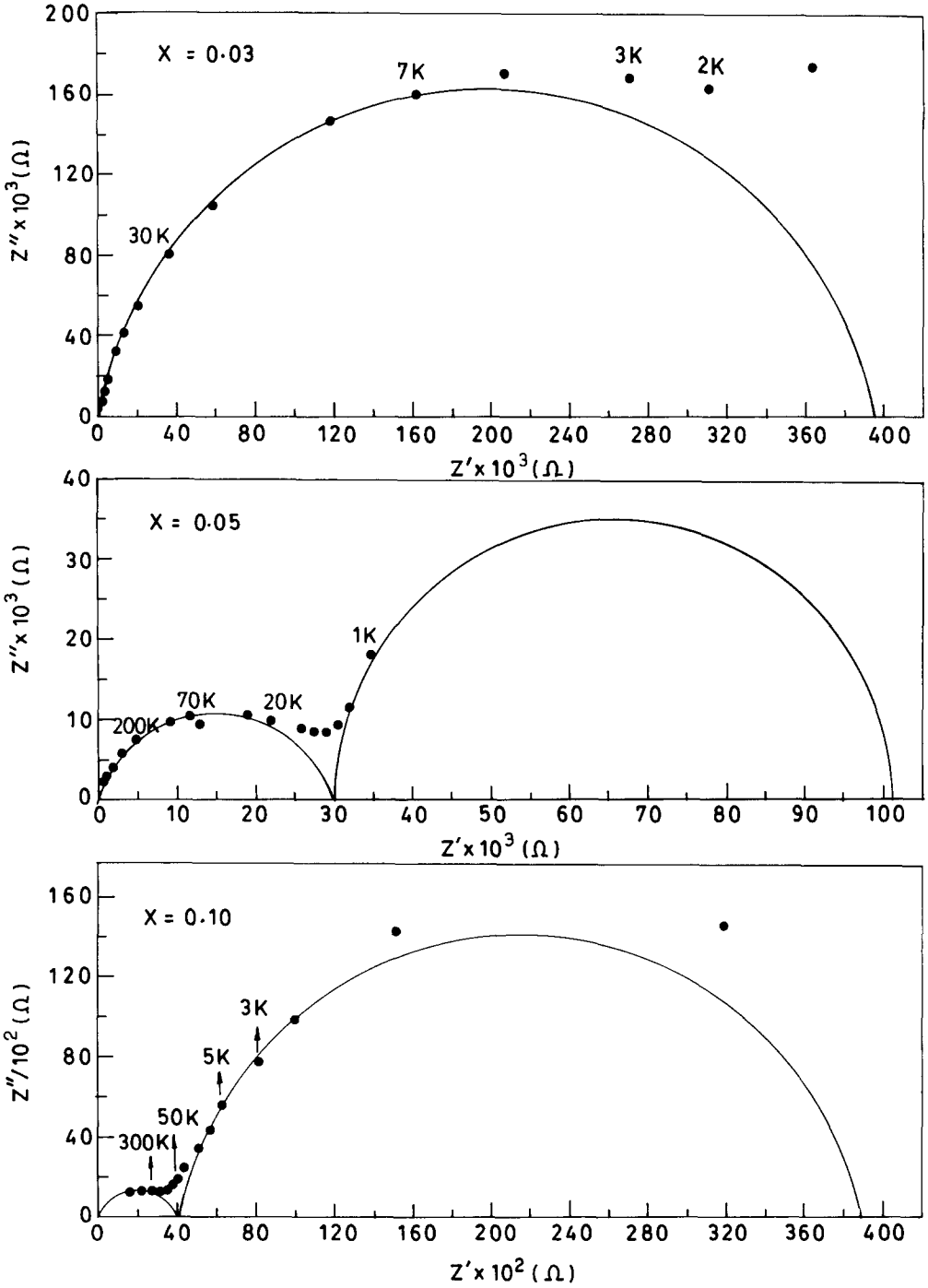

Fig. 1. Impedance plots of various compositions at 450 K in the $Sr_{1-x}La_xTi_{1-x}Ni_xO_3$ system.

frequency arc. The impedance data have been fitted manually. There may be some uncertainty in the resistance values obtained. However, since finally we are plotting the logarithm of resistivity as a function of temperature to find the activation energy of conduction, the error involved in its values will be insignificant.

Plots of logarithm of log ρ *vs.* $1000/T$ for various samples are shown in Fig. 3. These plots are linear indicating that resistivity obeys an Arrhenius relationship:

$$\rho = \rho_0 \exp E_a/kT \qquad (2)$$

where E_a is the activation energy for conduction. Values of E_a obtained by least-square fitting of the data are given in Table 1. Two slopes are observed for the sample with $x = 0.03$, while all other samples show only one value of activation energy over the temperature range of measurements. It is noted from Fig. 3 that resistivity decreases with increasing nickel ion concentration. This shows that conduction is predominantly

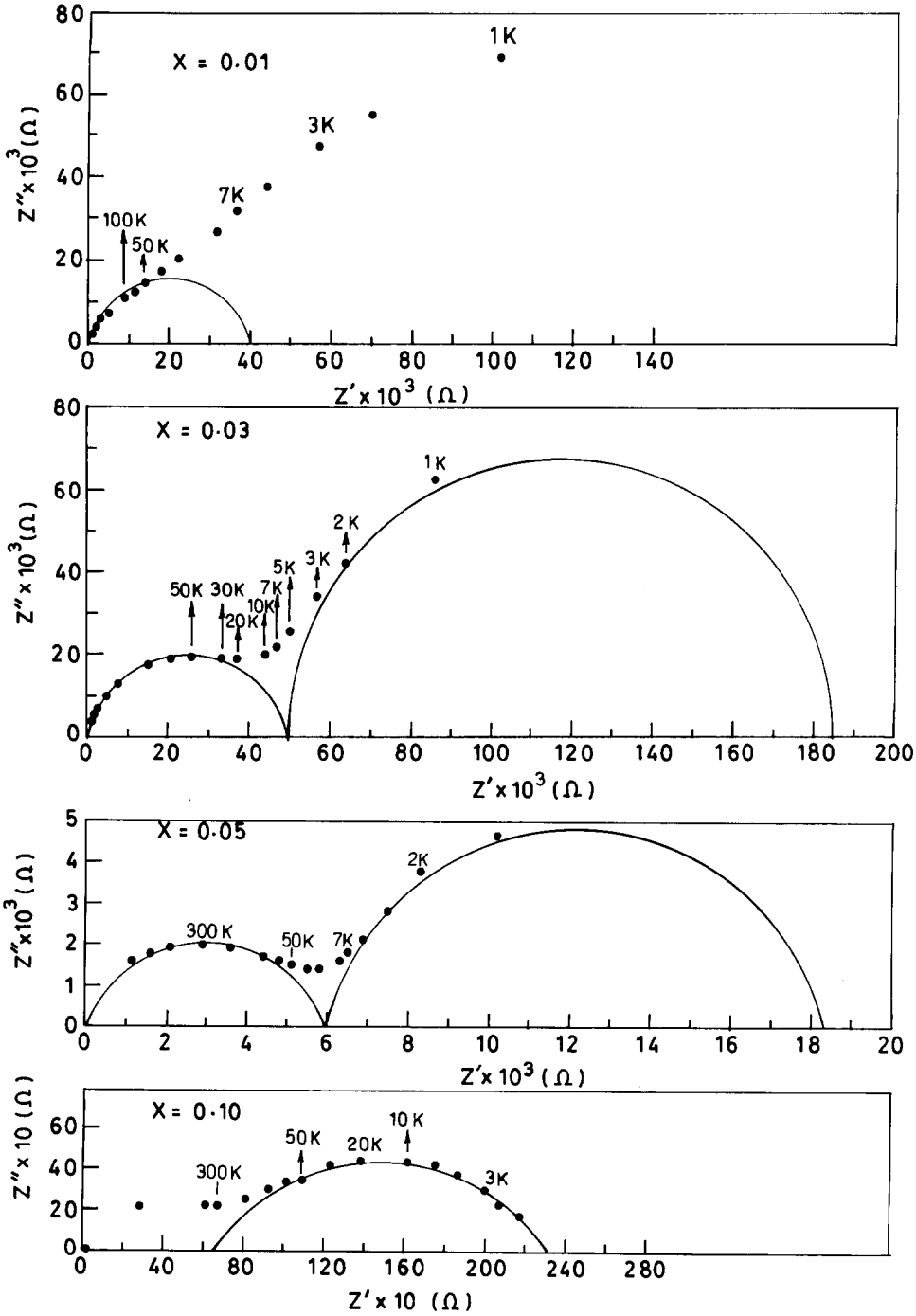

Fig. 2. Impedance plots of various compositions at 550 K in the $Sr_{1-x}La_xTi_{1-x}Ni_xO_3$ system.

due to nickel ions. The value of activation energy for conduction, E_a, decreases with increasing x. The values of E_a for the sample with $x=0.05$ and 0.10 are almost equal.

The band structure of $SrTiO_3$ consists of a filled valence band of 2p orbitals of oxygen ions separated by a band gap of ~3.2 eV from the empty conduction band of 4s orbitals of Ti^{4+} ions [20]. Nickel ions give rise to localized energy levels in the band gap at ~1.0 eV above the valence band similar to that in Ni-doped TiO_2 [21]. Conduction in pure $SrTiO_3$ has been explained as being due to hopping of small polarons between Ti^{3+} and Ti^{4+} sites [22]. In the present system conduction seems to occur by hopping of charge carriers among localized Ni^{2+} and Ni^{3+} sites. The presence of Ni^{2+} ions is explained as follows.

These materials are expected to lose traces of oxygen during sintering at high temperatures according to the reaction:

$$O_O \longrightarrow 1/2\ O_2 + V_O^{\cdot\cdot} + 2e' \qquad (3)$$

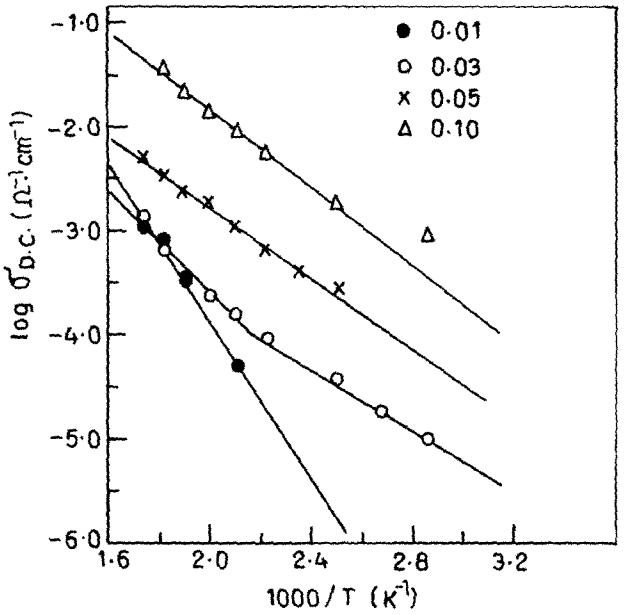

Fig. 3. Plots of log σ_{DC} *vs.* 1000/T for various compositions in the $Sr_{1-x}La_xTi_{1-x}Ni_xO_3$ system.

TABLE 1. Activation energy for DC conductivity (E_a) and AC conductivity (E'_a) at high temperature and E''_a at low temperature and hopping energy W_H for various samples in the $Se_{1-x}La_xTi_{1-x}Ni_xO_3$ system

x	E_a (eV)	E'_a (eV)	E''_a (eV)	W_H (eV)
0.01	0.74	0.38	0.04	0.36
0.03	0.50	0.30	0.09	0.20
0.05	0.33	0.30	0.15	0.03
0.10	0.37	0.28	0.20	0.09

where all the species are written as per Kroger Vink Notation of defects [23]. The electrons released in the process [3] are captured by Ni^{3+} to produce Ni^{2+} ions. Conduction then occurs due to hopping of electrons between Ni^{2+} and Ni^{3+} sites. The electrons released in the reaction may also be captured by Ti^{4+} to produce Ti^{3+}. However, this probability is very small as Ti^{4+} ions having inert gas configuration represent the most stable oxidation state of titanium ion in air.

In order to understand the mechanism of conduction, AC conductivity was measured as a function of frequency. Plots of log σ_{AC} *vs.* log f at a few temperatures for all the compositions are shown in Figs. 4 and 5. It is observed that AC conductivity varies with angular frequency as ($\omega = 2\pi f$)

$$\sigma_{ac} = A\omega^s \tag{4}$$

where s is a weak function of frequency at a given temperature. The values of s found by least-square fitting of the data are found to be in the range 0.4–0.6

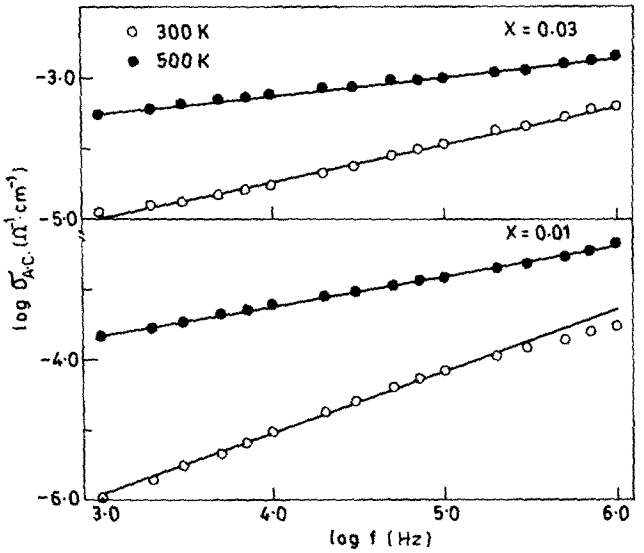

Fig. 4. Plots of log σ_{AC} *vs.* log f for $x = 0.01$ and $x = 0.03$ in the $Sr_{1-x}La_xTi_{1-x}Ni_xO_3$ system.

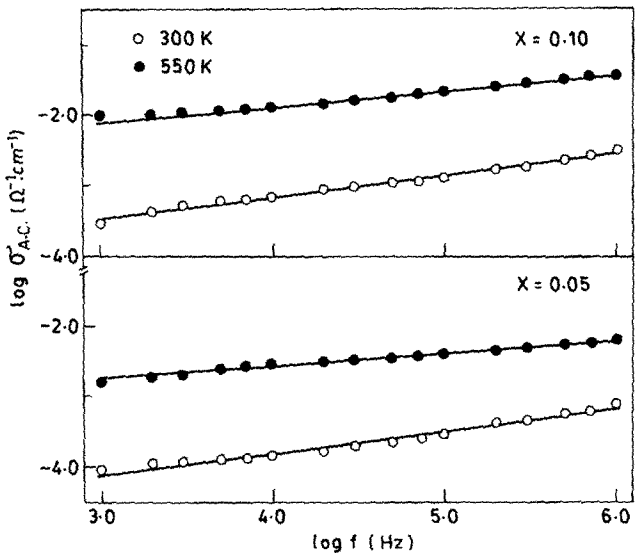

Fig. 5. Plots of log σ_{AC} *vs.* log f for $x = 0.05$ and $x = 0.10$ in the $Sr_{1-x}La_xTi_{1-x}Ni_xO_3$ system.

at 300 K. The value of s decreases with an increase in the temperature for a given composition.

Plots of logarithm of AC conductivity, σ_{AC}, at 100 KHz *vs.* 1000/T for all the compositions are shown in Fig. 6. We have plotted the data for AC conductivity at 100 KHz so that it has only a contribution from the bulk of the samples. Two regions are observed in these plots (a) a low temperature region in which the slope is less than and (b) a high temperature region in which the slope is greater than log σ_{AC} which varies linearly with 1000/T. Values of activation energies E'_a and E''_a calculated by least-square fitting of the data in these regions are given in Table 1.

The frequency dependence of AC conductivity given by eqn. (4) may be due to the following mechanisms.

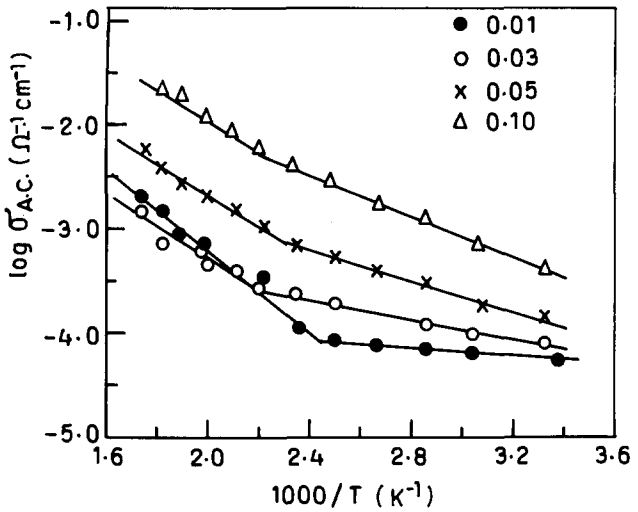

Fig. 6. Plots of log σ_{AC} *vs.* 1000/T for various compositions in the $Sr_{1-x}La_xTi_{1-x}Ni_xO_3$ system at 100 KHz.

1. At low temperatures, conduction seems to be by a Debye-type loss mechanism due to thermally activated hopping of charge carriers between two localized sites at a distance R [24, 25]. In this, a material containing N sites per unit volume, each having a dipole D, which can point in two or more directions with different energies W_1 and W_2 ($\Delta W = W_1 - W_2$) is considered. Both ΔW and τ (relaxation time) vary over a wide range including zero. Considering the hopping of an electron between two localized sites as thermally activated rotation of dipole, as in the above-mentioned Debye model, the expression for the frequency dependence of conductivity is:

$$\sigma(\omega, T) = A\ (e^2/\alpha^5)\ [N(E_F)]^2\ KT\omega[\ln(\nu_{ph}/\omega)]^4 \qquad (5)$$

where $A = (\pi^2/24)\ln 2 = 0.3$, α^{-1} is the radius of the localized wave function, ν_{ph} is a characteristic phonon frequency and $N(E_F)$ is the density of states at the Fermi level. The frequency dependence predicted by eqn. (5) is given by:

$$\sigma(\omega) = \omega\ (\ln\ \nu_{ph}/\omega)^4 \qquad (6)$$

If we assume the value of ν_{ph} to be in the range 10^7–10^{13} Hz, the value of s in eqn. (4) will be in the range 0.4–0.8 at $\omega = 10^4\ s^{-1}$ as observed in our samples. It is noted from eqn. (5) that AC conductivity is directly proportional to absolute temperature. In the case of impurity conduction with very low compensation, $\sigma(\omega)$ is independent of T [26].

In our system, the electrons of nickel ions seem to be responsible for conduction. In the low temperature region, the AC conductivity may be due to hopping of charge carriers among localized sites by a process similar to (1) giving rise to frequency dependence of σ_{AC} as ω^s and very little temperature dependence.

2. At higher temperatures, the conduction by transport of carriers excited into localized states at the valence band edge and hopping at energies close to it seems to dominate over the conduction process 1. The frequency and temperature dependence of conductivity in such a case is given by [27]:

$$\sigma(\omega,T) = (\pi^3/96)e^3/\alpha^5 kT[N(E_A)]^2\omega \qquad (7)$$
$$\times \ln(\nu_{ph}/\omega)^4 \exp\ -(E_F - E_A)/kT$$

The variation of DC resistivity for this mechanism is given by

$$\rho = \rho_0 \exp\ (E_F - E_A + W_H)/kT \qquad (8)$$

where E_A represents the valence band edge and W_H is the activation energy for hopping. For this mechanism both AC and DC conductivities vary exponentially with temperature. However, the activation energies for AC and DC conductivities are different. The difference between these two values gives the activation energy for hopping. In the higher temperature region, the observed frequency dependence of σ_{AC} given by eqn. (4) and its exponential temperature dependence shows that the transport occurs by this mechanism. The value of W_H for various compositions are given in Table 1.

3. Hopping of charge carriers among localized sites near the Fermi energy E_F will also give frequency and temperature dependence of AC conductivity similar to that given by process 1. However, in the present samples, process 1 is more probable than process 3 in the low temperature region because of polarization effects associated with the hopping of charge carriers. Ni^{+3} and Ni^{+2} ions on the Ti^{+4} site in this system form dipoles with positively charged oxygen vacancies $V_O^{\cdot\cdot}$. These dipoles can change their orientation by hopping of electrons between Ni^{+2} and Ni^{+3} sites. Thus conduction seems to occur by a Debye-type loss process at low temperature and by excitation of charge carriers at the valence band edge and hopping at energies close to it. The conduction process in this system is similar to that in $Ba_{1-x}La_xTi_{1-x}Ni_xO_3$ [19].

Acknowledgments

Financial support from Department of Science and Technology, Government of India, is gratefully acknowledged.

References

1 P.M. Raccah and J.B. Goodenough, *Phys. Rev., 155* (1967) 932.
2 V.G. Bhide, D.S. Rajoria, G. Rama Rao and C.N.R. Rao, *Phys. Rev., B6* (1972) 1021.

3 D.W. Meadowcroft, *Nature, 226* (1970) 847.
4 R.J.H. Voorhoeve, D.W. Johnson Jr., J.P. Remeika and P.K.G. Gallagher, *Science, 197* (1977) 827.
5 C.S. Tedmon Jr., H.S. Spacil and S.P. Mitoff, *J. Electrochem. Soc., 116* (1969) 1170.
6 O. Yamamoto, Y. Takeda, R. Kanno and M. Noda, *Solid State Ionics, 22* (1987) 241.
7 G. Goodman, in R.C. Buchanan (ed.), *Ceramic Materials for Electronic Applications*, Marcel Dekker, New York, 1986, pp. 79–138.
8 M.E. Lines and A.M. Glass, *Principle and Applications of Ferroelectrics and Related Materials*, Clarendon Press, Oxford, 1977, Chapter 12.
9 O. Parkash, Ch.D. Prasad and D. Kumar, *Phys. Stat. Solidi (a), 106* (1988) 627.
10 O. Parkash, Ch.D. Prasad and D. Kumar, *J. Mater. Sci., 25* (1990) 487.
11 O. Parkash, Ch.D. Prasad and D. Kumar, *J. Mater. Sci., 26* (1991) 6063.
12 O. Parkash, H.S. Tewari, L. Pandey, R. Kumar and D. Kumar, *J. Am. Ceram. Soc., 72* (1989) 1520.
13 O. Parkash, L. Pandey, M.K. Sharma and D. Kumar, *J. Mater. Sci., 24* (1989) 4505.
14 P. Ganguli and C.N.R. Rao, *Mater. Res. Bull., 8* (1973) 405.
15 I.M. Hodge, M.D. Ingram and A.R. West, *J. Electroanal. Chem., 74* (1976) 125.
16 A. Hooper, *J. Phys. D: Appl. Phys., 10* (1977) 1487.
17 A.R. Von Hipple, in *Dielectric and Waves*, John Wiley and Sons, London, 1954, p. 191.
18 H.S. Maiti and R.N. Basu, *Mater. Res. Bull., 21* (1987) 1107.
19 O. Parkash, H.S. Tewari, V.B. Tare and D. Kumar, *J. Alloy Comp., 190* (1993) 243.
20 A. Linz, *Phys. Rev., 91* (1953) 753.
21 K. Mizushima, M. Tanaka and S. Lida, *J. Phys. Soc. Jpn., 32* (1972) 1519.
22 D. Parker and J. Yahia, *Phys. Rev., 169* (1968) 605.
23 I. Burn and S. Neirman, *J. Mater. Sci., 17* (1982) 3510.
24 M. Pollak and T. Geballe, *Phys. Rev., 122* (1961) 1742.
25 I.G. Austin and N.F. Mott, *Adv. Phys., 18* (1969) 41.
26 N.F. Mott and E.A. Davis, *Electronic Processes in Non-Crystalline Materials*, Oxford University Press, Clarendon Press, 1979, Chapter 6.
27 S.R. Elliot, *Phil. Mag., B37* (1978) 553.